



A novel modified U-shaped microstrip antenna for super wide band (SWB) applications

Mourad Elhabchi¹ · Mohamed Nabil Srifi² · Raja Touahni¹

Received: 22 November 2018 / Revised: 23 March 2019 / Accepted: 23 January 2020 / Published online: 28 January 2020
© Springer Science+Business Media, LLC, part of Springer Nature 2020

Abstract

In this work, a novel wideband microstrip modified slotted U-shaped printed monopole antenna operating from 3 to 20 GHz for super-wideband applications is proposed. To have an effect on the enhancement of bandwidth and to get better impedance matching over the frequency band, three modifications are introduced, the first one is to print two symmetric triangular shaped slots in the radiating element and the second one is to modify the partial rectangular ground plane to be defected ground plane by slotting three triangular structures. The third modification is to embed a circular slot in the center of the patch for integrating the entire FCC band (3.1–10.6 GHz) in the super wide band antenna. Both CST Microwave Studio and Ansoft HFSS 3-D EM solver were used for the simulation analysis of antennas while measurements after fabrication are performed by applying ZVB 20—vector network analyzer 20 MHz–20 GHz. The average maximum gain of the antenna is 5.72 dB with good radiation patterns. The antennas have only been measured up to 20 GHz (the upper frequency limit of the laboratory vector network analyzer device), simulations results both in CST and HFSS shows satisfactory design's performance up to 40 GHz. So as this antenna is a candidate to fulfil the future UWB spectrum requirements in a very wide band. A good agreement between the measured and simulated results is achieved in term of return loss in the measured band (up to 20 GHz).

Keywords U-shaped · Super wide band · Bandwidth · Triangular-shaped-slots · Defected ground plane · Circular slot

1 Introduction

The rapid developments in the wireless communication systems improve the demand of the Ultrawideband (UWB) antenna designs since February 2002 when the federal communications commission (FCC) unlicensed the 3.1–10.6 GHz band to be used for free [1]. In addition, UWB technology attracted more attention of the scientific

community and the industrial sectors owing to their promising characteristics such as high data rate useful for short range indoor communications and mobile handheld devices, good radiation pattern, good impedance matching performance, low complexity and fabrication cost, low weight and it's simple to be integrated in the RF circuits [2]. The UWB antennas are recently being the interest components of UWB systems because it has been proven very popular and adequately efficient [3]. To enhance the bandwidth features of a printed antenna, several techniques have been previously presented and investigated such as using different radiator shapes and slots [4, 5], feeding methods [6] and polarisation diversity [7]. A stacked parasitic strips based on LTCC technology are used to enhance the bandwidth and gain of patch Antenna [8], the variable band-stop function is obtained by slotting an inverted T-shaped at the square radiating stub to create an additional resonances frequency [9]. The UWB spectrum properties of the presented in antenna [10] are achieving using dielectric resonator coupled with chaotic oscillator with

✉ Mourad Elhabchi
mouradelhabchi@hotmail.fr

Mohamed Nabil Srifi
srifimn@ieee.org

Raja Touahni
touahni-raja@univ-ibntofail.ac.ma

¹ LASTID Laboratory, Department of Physics, Faculty of Sciences, Ibn Tofail University, Kenitra, Morocco

² Electronics and Telecommunication Systems Research Group, National School of Applied Science (ENSA), Ibn Tofail University, Kenitra, Morocco

high isolation. Khalili et al. [11] investigated a P-Shaped DRA design to obtain a wide band antenna suitable for wireless communication applications. A fractal structure is used to improve the bandwidth of CPW-fed UWB monopole and hexagonal antennas. Fallahi and Atlasbaf have been loaded the CPW-fed monopole antenna with a number of small fractal polygons shaped elements to enhance the bandwidth [12]. Sawant and Kumar have been proposed a CPW hexagonal fractal structure loaded with 41 hexagons shaped to make fractal geometry and to improve UWB features [13]. Gautam et al. extends the two sides of the ground plane vertically to obtain an UWB behavior of minimizing monopole CPW hexagonal shape [14], a multiple input multiple output (MIMO) antenna is also implemented and analyzed for creating UWB response. Ahmed et al. designed and investigated a super-wideband (SWB) MIMO antenna with high isolation, operating from 3.1 to 20 GHz, with the inclusion of L-shaped strip in the ground plane with defined positions and dimensions [15]. Huang and Guang Xiao concepts a compact diversity polarization MIMO antenna using linear tapered slot with fork-shaped and two orthogonal feed lines to achieve the UWB characteristics [16] and so on. By using these techniques, desired operating bandwidth ranges can be achieved.

In this paper a new shape of miniaturized super wide band (SWB) antenna has been investigated and manufactured. The main objectives of this work is to obtain a very wide band, high gain, in single compact structure of $30 \times 30 \text{ mm}^2$ based on the printed monopole configuration and referring to the prototype presented in [17].

The proposed structure consists of a modified U-shaped slotted by a symmetric triangular shaped both in the radiating patch and the ground plane, to improve the performance of the proposed structure and to create an additional resonance frequency we are also slotted two shaped, a concentric circle and a central triangle defected ground plane respectively in the patch and the ground plane. The final configuration of this antenna has a three shaped-slot on the patch and a three shaped-slot in the ground plane. The impedance bandwidth of the wideband response has covered the frequency range 3–20 GHz, which can be a candidate to fulfils the requirements of the very wide band for wireless devices.

2 Antenna design and analysis

2.1 Antenna configuration

The configurations of the proposed SWB antenna are shown in Fig. 1, together with its geometrical dimensions. This antenna is manufactured on a FR-4 substrate having a

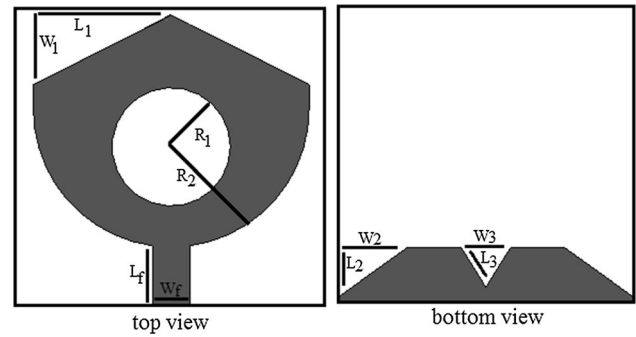


Fig. 1 The Geometry of the reconfigured SWB antenna, ($W_s = L_s = 30$, $W_f = 3$, $L_f = 6$, $R_1 = 6$, $R_2 = 14$, $W_1 = 7$, $L_1 = 14$, $W_2 = 5$, $L_2 = 5$, $W_3 = 2.5$, $L_3 = 4$) (Unit: millimeters)

dielectric substrate of 4.3, height of 1.6 mm and loss tangent of 0.025. The feeding system consists of a 50 Ω microstrip line for impedance matching. The presented design occupies a small area of $30 \times 30 \text{ mm}^2$, which is considerably less than competitive structures featuring similar bands and geometries. To determine the approximated value parameters of this antenna. Basic formulas and microwave calculator was used [18]. This SWB microstrip antenna is designed directly from the conventional U-shaped patch antenna with some modifications in the radiating structure and the ground plane to improve the bandwidth and the performance of the design. For getting resonance, total length and width of the radiating shaped is taken about half of the guided wavelength at 3 GHz.

The radius of the circular part of the radiating element is calculated for a height of 1.6 mm using the following equations [19] as well as the desired resonant frequency f_r of a circular patch antenna is approximately given:

$$f_r = \frac{Kc}{2\pi a_e \sqrt{\epsilon_r}} \quad (1)$$

In this paper $k = 1.84118$ for the fundamental mode TM_{11} a_e represent the effective radius of the circular patch. The expression of a_e for is:

$$a_e = a \left\{ 1 + \frac{2h}{\pi \epsilon_r a} \left[\ln \left(\frac{\pi a}{2h} \right) + 1.7726 \right] \right\}^{1/2} \quad (2)$$

ϵ_r is the relative permittivity of the dielectric. The radius of the circular patch is expressed as:

$$a = \frac{F}{\left\{ 1 + \frac{2h}{\pi \epsilon_r F} \left[\ln \left(\frac{\pi F}{2h} \right) + 1.7726 \right] \right\}^{1/2}} \quad (3)$$

The value of F can be calculated by the following equation:

$$F = \frac{8.791 \times 10^9}{f_r \sqrt{\epsilon_r}} \quad (4)$$

The circular radius of the proposed SWB antenna is $a = 7.5$ mm. Generally substrate length L and width W are taken two times larger than patch diameter ($2a$). So substrate length and width can be written as: $L_s = 2 \times 2a = 30$ mm and $W_s = 2 \times 2a = 30$ mm (Fig. 2).

In order to present the design procedure of the proposed SWB antenna, The evolution process step by step of our proposed geometry is shown in (Fig. 3).

The simulated frequency response of the return loss of the developed proposed SWB antenna step by step, is illustrated in Fig. 4. For the antenna denoted as (Ant I), it's the reference design and is forming a frequency band from 3 to 6 GHz with worse impedance matching, trace (I) indicates that the antenna cover only 3 GHz in the UWB response. As the center of the ground plane of the conventional design is defected by a triangular resonator slot and the radiating element is slotted with a two symmetric triangular shape (Ant II), the resonance becomes better than the first design, but without the integration of the entire FCC band (3.1–10.6 GHz),(trace II). As the radiating element is loaded with a concentric circular slot(Ant III), the UWB response is integrated except two bands (6–7 GHz) and (13–14 GHz),(trace III)). In order to improve the impedance matching conditions for covering the entire super wide band applications, a two symmetric triangular slots are loaded in the edge of the ground plane(Ant VI). Hence, the reflexion coefficient is now < -10 dBi (Trace VI) with good adaptation (Fig. 5).

2.2 Operating principle

Many modifications are introduced in the conventional antenna (Fig. 4 Ant I) for bandwidth enhancement. The first one is done by including two symmetric triangular slots in the U-shaped patch and a central triangular slot defected ground plane under the transmission line (Fig. 4 Ant II), The current path is changed and its distribution is increased, the second one is to load a wide circular slot in the patch for more antenna adaptation (Fig. 4 Ant III), this modifications are not significantly sufficient for getting an adaptive antenna, for that the authors are slotted two symmetric triangular defected ground structures shaped in

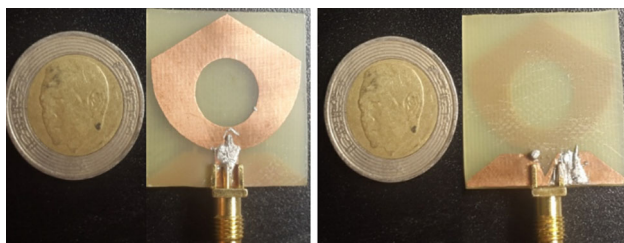


Fig. 2 Photographs of the fabricated antenna

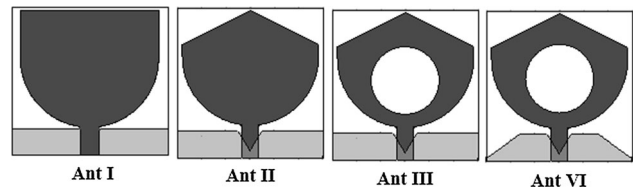


Fig. 3 The evolution of the proposed SWB antenna. Ant I (Step I). Ant I I(Step II)., Ant III (Step III). Ant VI (the proposed design)

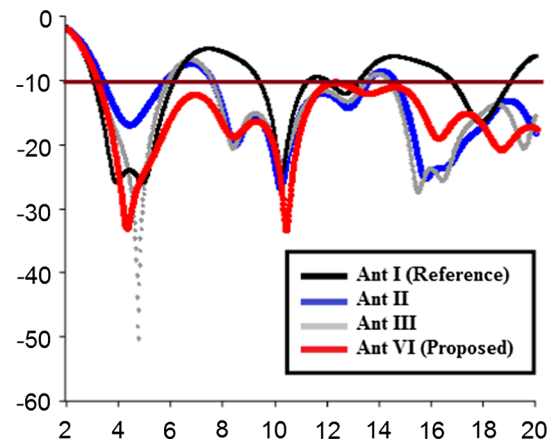


Fig. 4 Simulated S_{11} parameters of the proposed antenna with different structures

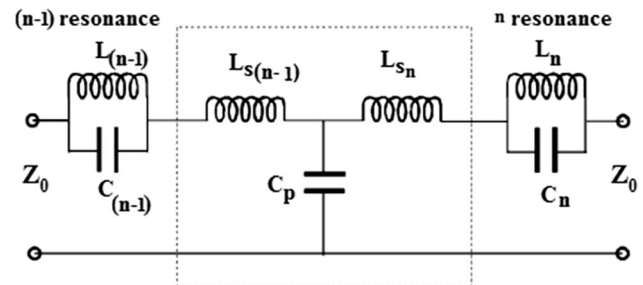


Fig. 5 General circuit model for the DGS

the left and right edges of the ground plane(Fig. 4 Ant VI). As a result, the effective capacitance and inductance changes of the antenna and the bandwidth were improved. The defects on the ground plane and the radiating element change the path of the current distribution in the slotted region. This current is enhanced due to the aperiodic triangular slots and circular slot parts of the modified U-shaped antenna. This effect changes the features of the antenna due to the variation of effective capacitance and inductance of microstrip line, ground plane and radiating patch element. The coupling with these slots are responsible for adding a capacitive effect and the central triangular ground plane slot connects both the U-shaped patch element with the DGS for adding the inductance to the total Impedance [20].

The inductance L_n and capacitance C_n are given as [21]:

$$L_n = \frac{1}{4\pi^2 f_{0n}^2 C_n} \quad \text{for } n = 1, 2, \dots \quad (5)$$

$$C_n = \frac{f_c}{2Z_0 2\pi (f_n^2 - f_{01}^2)} \quad (6)$$

$$C_P = \frac{1}{2\pi f_T X_{n(n-1)}} \quad (7)$$

$$L_{S_n} = \frac{X_{nn} - X_{n(n-1)}}{2\pi f_T} + \frac{L_i}{\left(\frac{f_T}{f_{0n}}\right)^2 - 1} \quad (8)$$

where f_n and f_{01} are respectively the resonant frequency at cut-off frequency of the n^{eime} resonance and de 1st resonance. $L_{S(n-1)}$ and L_{S_n} and C_P consisting of T-network witch represents the interaction between the two resonators. f_T is the transit frequency witch represent the frequency that below it the $(n-1)$ resonator dominates and above it the n^{eime} resonator dominates. Z_0 is 50 O characteristic impedance of the transmission line.

The resonant frequency of the circuit and the inductance L_n and capacitance C_n is given by equation [22]:

$$f_c = \frac{1}{2\pi\sqrt{L_n C_n}} \quad (9)$$

The development and studies of the circuit model give us an idea of the design parameter variation effects. The dielectric gap between conducting layers, leads to the generation of a parallel combination of capacitance C_n and conductance L_n . In this antenna, the parallel combinations of C_n , L_n , represent the equivalent models between conducting slotted radiating element and the ground plane of the n^{eime} resonants, respectively. The parallel capacitance with effective line inductance can be provided by the etched gap area placed under a conductor line. The series inductance due to the DGS section increases the reactance of a microstrip with the increasing of the frequency while the reactance of the capacitance decreases [23].

The isosless triangular slots in the ground plane and the patch structure serves as to provide a better impedance matching for the antenna. The inductors $L_{S(n-1)}$ and $L_{S(n)}$ account some inductance due to fringing fields and surface waves. The variation in capacitance between the antenna elements leads to a variation of the electrical field of the proposed structure. Due to negligible current density in the ground plane than the patch structure. The series combination of R and L as well as the parallel combination of capacitance C and conductance G between the connected feed line and the bottom edge of the proposed SWB design cannot affect in the antenna performance it's can be neglected. The parallel capacitance with the series inductance provides the attenuation pole location and started the elimination of the certain frequency signals of the proposed SWB DGS, which is the multiple successive resonance

frequencies of the parallel L_n and C_n resonators, the mode of propagation of wave is considered to be purely TEM. Hence, the bandwidth of the antenna can be enhanced due to current distributions in two diverse paths after the feed line in the high signal region, small changes for the characteristic impedance (the impedance of the transmission line becomes more than 200 ohms), the inductance, (will increase and at the same time the capacitance will be decreased) and the effective dielectric constant (the band gap effect).

2.3 Parametric studies of the SWB antenna

Figure 6. Depict the simulated reflexion coefficient traces for different values of R_1 witch represent the radius of the resonator circle slot. As observed, the resonance band is shifted to the lower frequency and the reflexion coefficient increases from -15 to -9 dBi when the value of R_1 increases from 2 to 8 mm. The good value to ensure good adaptation in the desired SWB band is $R_1 = 6$ mm.

Figures 7 and 8 show the effect of the width and length of the two symmetric triangular defected ground plane slots (W_2 , L_2). As illustrated in these figures by increasing W_2 and L_2 , the impedance matching is improved, especially at high and low frequencies for W_2 and L_2 respectively, so the proper values of W_2 and L_2 to achieve SWB response are $W_2 = 5$ mm and $L_2 = 5$ mm. On the other hand, increasing W_3 and L_3 parameters leads to shift the curves of S_{11} from the worse impedance matching $S_{11} > -10$ dBi to the good impedance matching $S_{11} < -10$ dBi as shown in (Figs. 9 and 10).

The optimum dimensions of W_3 and L_3 when the antenna is suitable for SWB applications are $W_3 = 2.5$ mm and $L_3 = 4$ mm.

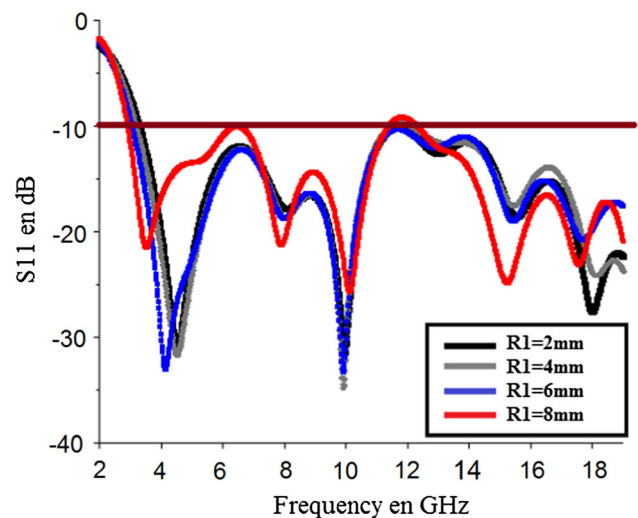


Fig. 6 S_{11} parameters for different circular slot shaped radius R_1

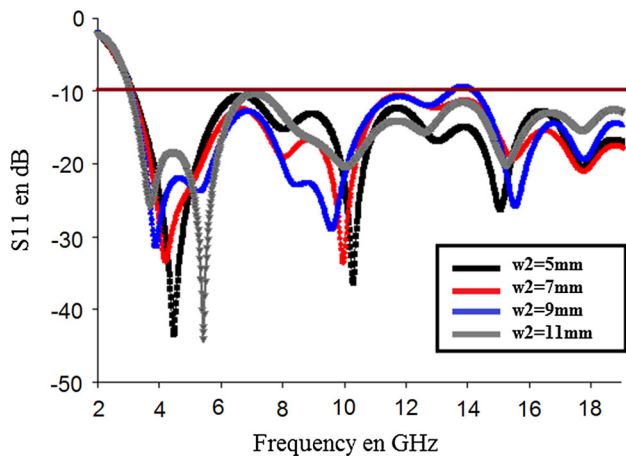


Fig. 7 S_{11} parameters for different triangular slot shaped width W_2

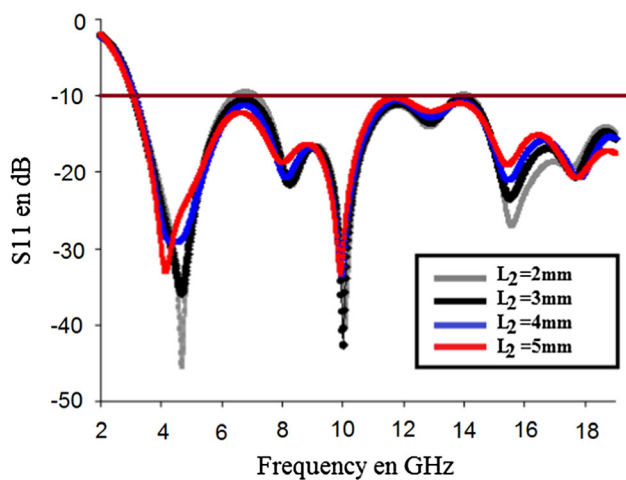


Fig. 8 S_{11} parameters for different triangular slot shaped length L_2

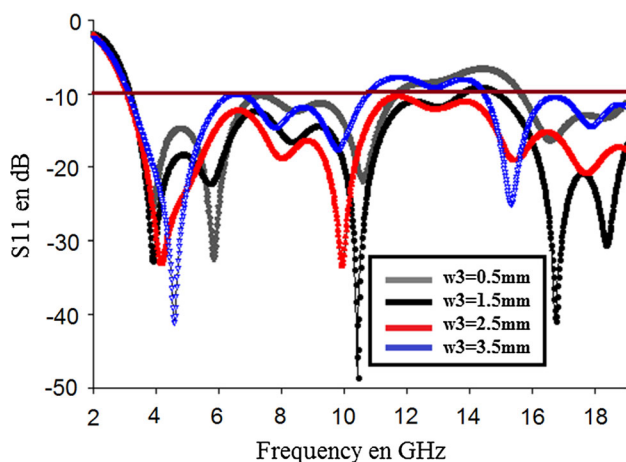


Fig. 9 S_{11} parameters for different triangular slot shaped width W_3

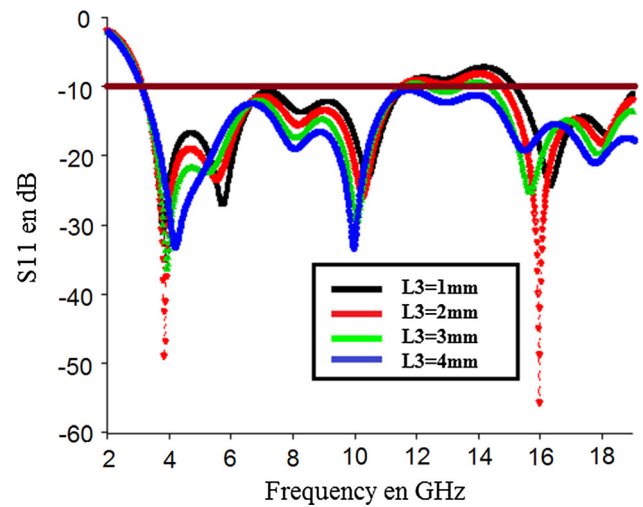


Fig. 10 S_{11} parameters for different triangular slot shaped length L_3

3 Simulated current distribution

The simulated current distributions on the proposed SWB antenna at 3.5, 5.5, 10, and 16.5 GHz are shown in Fig. 11.

The Current distribution is mainly concentrated on the edges of the interior and exterior of the triangle and circular resonator slots. Therefore, the antenna impedance matching affected at this frequency due to the resonant property of the loaded slots in the radiating stub and the ground plane. As a result, the resonator slots are considered as a major part of achieving SWB response [24].

3.1 Simulated 3D gain

Figure 12 depicts 3D plots of gain values for the prototype SWB antenna at each selected frequency of 3.5, 5.5 GHz. As a result, the antenna has acceptable gain at

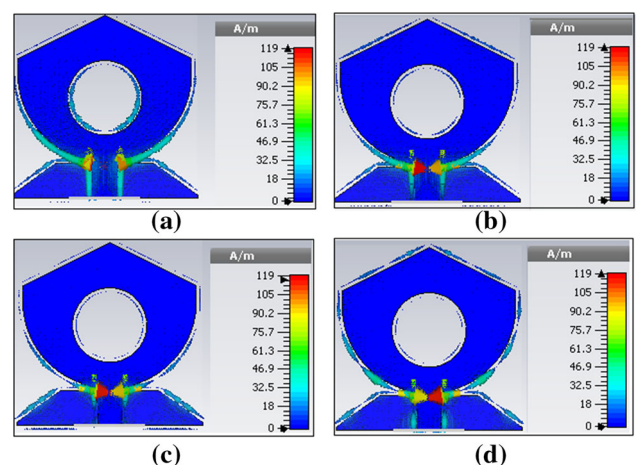


Fig. 11 Current distributions at a 3.5 GHz, b 5.5 GHz, c 10 GHz, and d 16.3 GHz

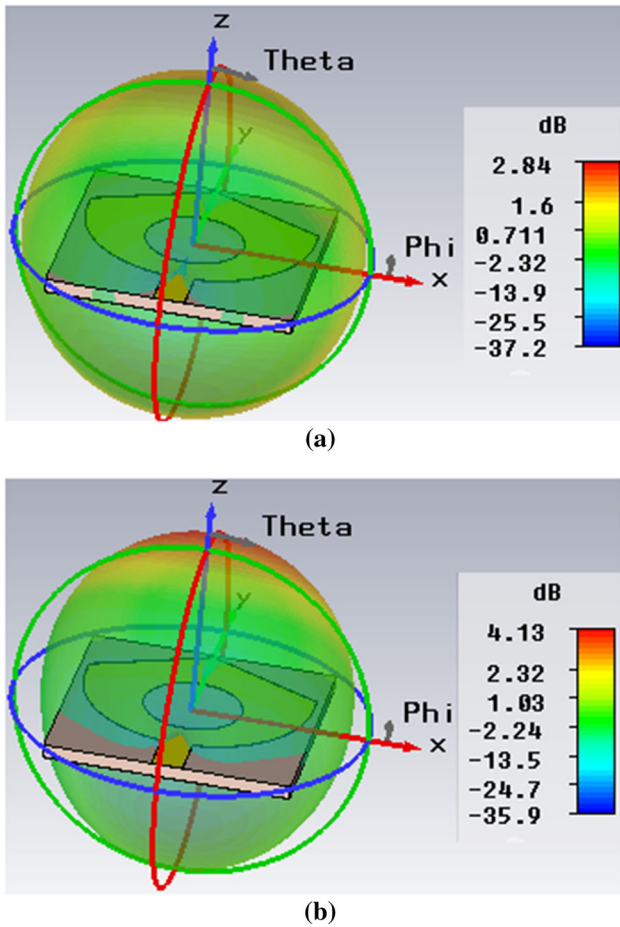


Fig. 12 Simulated radiation patterns at a 3.5 GHz, b 5.5 GHz

these frequencies and could be attractive for current and UWB applications [25].

3.2 Simulated radiation patterns

The simulated farfield radiation patterns both in CST microwave and Ansoft HFSS softwares on E-plane and H-plane are depicted in Figs. 13(a) and (b) at 3.5 GHz and 5.5 GHz respectively. From the traces observed in these figures, bidirectional radiation patterns are shown for both E-plane and H-plane for selected operating frequency bands.

As a result. The antenna has acceptable radiation coverage.

4 Measurement results and discussion

Simulated and measured reflexion coefficient parameters are shown in Fig. 14. The prototype SWB antenna is manufactured, and the S_{11} parameters are measured by

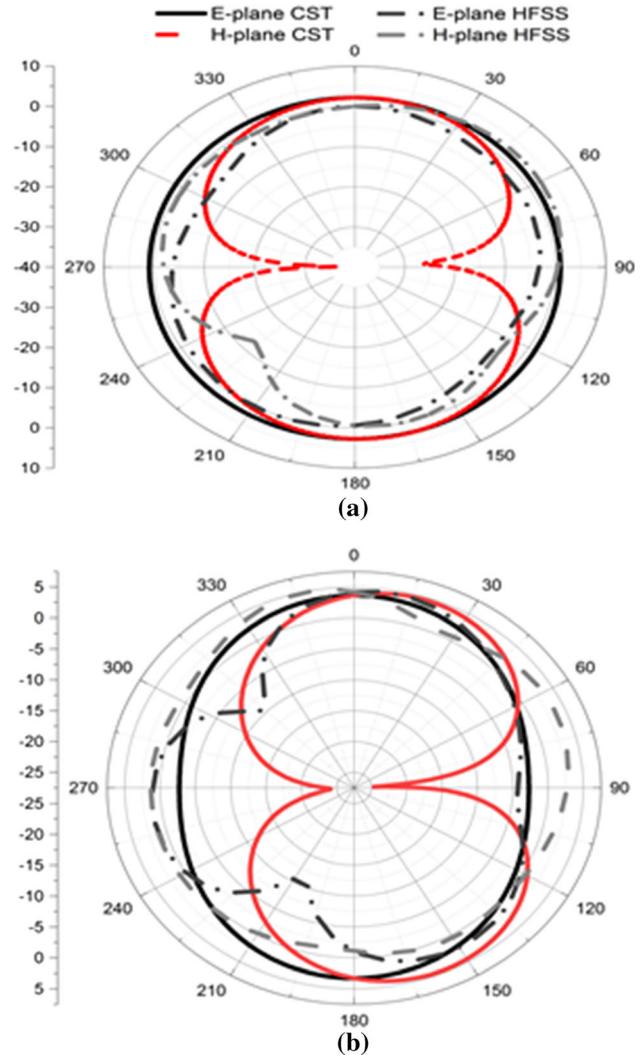


Fig. 13 Simulated radiation patterns at a 3.5 GHz, b 5.5 GHz

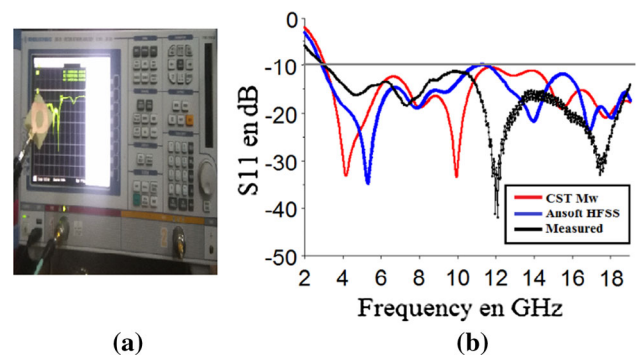


Fig. 14 a The proposed antenna under test. b Simulated and measured S_{11} parameters

using the ZVB 20—Vector Network Analyzer 20 MHz–20 GHz.

The measured results closely in good agreement with the simulated ones.

Table 1 Comparison between the performance of some recently developed UWB designs and the proposed design

Antenna	Bandwidth(GHz)	Antenna size (mm ²)	Gain (dB)
This work	3–20	30 × 30	2.84–6
Ref. [2]	2.5–12	50 × 50	Not defined
Ref. [3]	2.25–12.8	30 × 35	2–5.7
Ref. [4]	3–14	35 × 30	2–4.5
Ref. [7]	3.85–11.85	20 × 28	1.2–3.2
Ref. [9]	2.9–17.1	20 × 20	2–5
Ref. [11]	3.5–8	17 × 35	Not defined
Ref. [12]	3.1–10.6	25 × 25	1–3.2
Ref. [14]	2.71–12.61	25 × 23	Not defined
Ref. [15]	3.1–20	93 × 56	Not defined
Ref. [16]	3.1–12	32 × 32	< 4
Ref. [17]	3–6	30 × 30	< 5.6
Ref. [24]	4.56–13.1	16 × 12	1–4.8

5 Comparison between recently designed antennas and the proposed antenna

Table 1 presents a comparison between the performance of some recently studied UWB designs and the proposed design. The proposed antenna shows good achievement of SWB response, compact size, and acceptable gain characteristics in a very wide band.

6 Conclusion

In this letter, a novel compact super wide band SWB antenna has been successfully designed and optimized using different resonator slots for bandwidth enhancement of the conventional U-shaped antenna. The bandwidth was achieved through triangular and circular slot resonators loading onto the radiating element and the ground plane of the reference antenna led to a very wide band from 3 to 20 GHz with a reasonable maximum gain value without increasing their size. Experimental validation confirms the correctness of the design approach in the measured band. Finally, this proposed technique is very simple to introduce in practice and can be candidate to fulfils the requirements of the very wide band for future wireless devices.

Acknowledgements The authors would like to thank team of the Laboratory of Information System and Telecommunications, Abdelmalek Essaâdi University for their support to carry out the measurement of this work.

References

1. Federal Communications Commission. (2002). *Revision of part 15 of the commissions rules regarding ultra-wide-band transmission systems first report and order FCC 02. V48*, Washington, DC, Technical Report
2. Vendik, I. B., Rusakov, A., Kanjanasit, K., Hong, J., & Filonov, D. (2017). Ultra-wideband (UWB) planar antenna with single-, dual-, and triple-band notched characteristic based on electric ring resonator. *IEEE Antennas and Wireless Propagation Letters*, *16*, 1597–1600.
3. Ebadzadeh, S. R., & Zehforoosh, Y. (2017). A compact UWB monopole antenna with rejected WLAN band using split-ring resonator and assessed by analytic hierarchy process method. *Journal of Microwaves, Optoelectronics and Electromagnetic Applications*, *16*(2), 592–601.
4. Liang, X. L., & Denidni, T. A. (2008). H-shaped dielectric resonator antenna for wideband applications. *IEEE Antennas Wireless Propagation Letters*, *7*, 163–166.
5. Denidni, T. A., Rao, Q., & Sebak, A. R. (2005). Broadband L-shaped dielectric resonator antenna. *IEEE Antennas and Wireless Propagation Letters*, *4*, 453–454.
6. Mandal, T., & Das, S. (2013). Microstrip feed spanner shape monopole antennas for ultra wide band applications. *Journal of Microwaves, Optoelectronics and Electromagnetic Applications*, *12*(1), 15–22.
7. Nikolaou, S., & Abbasi, M. A. B. (2017). Design and development of a compact UWB monopole antenna with easily-controllable return loss. *IEEE Transactions on Antennas and Propagation*, *65*(4), 2063–2067.
8. Li, L., Zhang, Y., Wang, J., Zhao, W., Liu, S., & Xu, R. (2014). Bandwidth and gain enhancement of patch antenna with stacked parasitic strips based on LTCC technology. *International Journal of Antennas and Propagation*, Article ID 461423.
9. Mazloun, J., Parchin, N. O., & Ojaroudi, S. (2017). Bandwidth enhancement of small slot antenna with a variable band-stop function. *Wireless Personal Communications*, *95*(2), 1147–1158.
10. Kumari, B., & Gupta, N. (2018). UWB active antenna using dielectric resonator. *Microwave and Optical Technology Letters*, *60*(8), 1894–1898.
11. Khalily, M., Rahim, M. K. A., Kishk, A. A., & Danesh, S. (2013). Wideband P-shaped dielectric resonator antenna. *Radioengineering*, *22*(1), 281–285.
12. Fallahi, H., & Atlasbaf, Z. (2015). Bandwidth enhancement of a CPW-fed monopole antenna with small fractal elements. *AEU - International Journal of Electronics and Communications*, *69*, 590–595.
13. Sawant, K. K., & Kumar, C. S. (2015). CPW fed hexagonal micro strip fractal antenna for UWB wireless communications. *AEU-International Journal of Electronics and Communications*, *69*(1), 31–38.
14. Gautam, A. K., Chandel, R., & Kr Kanaujia, B. (2013). A CPW-fed hexagonal-shape monopole-like UWB antenna. *Microwave and Optical Technology Letters*, *55*(11), 2582–2587.
15. Ahmed, B. T., Olivares, P. S., Campos, J. L. M., & Vázquez, F. M. (2018). (3.1–20) GHz MIMO Antennas. *International Journal of Electronics and Communications*, *94*, 348–358.
16. Huang, H. F., & Xiao, S. G. (2017). A compact polarization diversity UWB MIMO antenna with a fork-shaped decoupling structure. *Progress In Electromagnetics Research Letters*, *69*, 87–92.
17. Jangid, K. G., Jain, P. K., Sharma, B. R., Saxena, V. K., Kulhar, V. S., & Bhatnagar, D. (2017). Ring slotted circularly polarized U-shaped printed monopole antenna for various wireless applications. *Advanced Electromagnetics*, *6*(1), 70–76.

18. Mythili, P., & Das, A. (1998). Simple approach to determine resonant frequencies of microstrip antennas. *IEEE Proceedings-Microwaves, Antennas and Propagation*, 145(2), 159–162.
19. Ray, K. P., & Kumar, G. (1999). Determination of the resonant frequency of microstrip antennas. *Microwave and Optical Technology Letters*, 23(2), 114–117.
20. Hong, J. S., & Karyamapudi, B. M. (2005). A general circuit model for defected ground structures in planar transmission lines. *IEEE Microwave and Wireless Components Letters*, 15(10), 706–708.
21. Singhal, S. (2017). Asymmetrically fed octagonal Sierpinski band-notched super-wideband antenna. *Journal of Computational Electronics*, 16(1), 210–219.
22. Khandelwal, M. K., Kanaujia, B. K., & Kumar, S. (2017). Defected ground structure: Fundamentals, analysis, and applications in modern wireless trends. *International Journal of Antennas and Propagation*, 2017, 2018527. <https://doi.org/10.1155/2017/2018527>.
23. Taher, H. (2012). A simplified equivalent circuit model for defected ground structures in planar transmission lines. *Progress In Electromagnetics Research Letters*, 29, 157–166.
24. Singhal, S., & Singh, A. K. (2017). Asymmetrically CPW-fed ladder-shaped fractal antenna for UWB applications. *Analog Integrated Circuits and Signal Processing*, 92(1), 91–101. <https://doi.org/10.1007/s10470-017-0976-5>.
25. Li, X., Xu, Y., Wang, H., Zhang, Y., & Lv, G. (2018). Low cross-polarization antipodal tapered slot antenna with gain bandwidth

enhancement for UWB application. *Journal of Computational Electronics*, 17(1), 442–451.

Publisher's Note Springer Nature remains neutral with regard to jurisdictional claims in published maps and institutional affiliations.



Mourad Elhabchi was born in Sidi Slimane, Morocco, in April 1987. He received the Licence de Physique degree in electronics from Ibn Tofail University, Kenitra, Morocco, in 2009, and the Deep Higher Studies Diploma Master degree in telecommunications systems from Abdelmalek Essaadi University Tetuan, Morocco, in 2013 and he is currently the Ph.D. Student in LASTID Laboratory, Faculty of Sciences Ibn Tofail University, He is the

author of more than 3 papers which appeared in refereed specialized international journals and conferences.